APPLIED AND ENVIRONMENTAL MICROBIOLOGY, Feb. 2011, p. 1069–1075 Vol. 77, No. 3
0099-2240/11/$12.00 doi:10.1128/AEM.02912-09

Microbial Communities and Electrochemical Performance of Titanium-Based Anodic Electrodes in a Microbial Fuel Cell[▽]

Urania Michaelidou,[1,2]* Annemiek ter Heijne,[1,3] Gerrit Jan W. Euverink,[1] Hubertus V. M. Hamelers,[3] Alfons J. M. Stams,[2] and Jeanine S. Geelhoed[2,4]

Wetsus, Centre of Excellence for Sustainable Water Technology, Agora 1, P.O. Box 1113, 8900 CC Leeuwarden, Netherlands[1]; Laboratory of Microbiology, Wageningen University, Dreijenplein 10, 6703 HB Wageningen, Netherlands[2]; Sub-department of Environmental Technology, Wageningen University, Bomenweg 2, P.O. Box 8129, 6700 EV Wageningen, Netherlands[3]; and Max Planck Institute for Marine Microbiology, Celsiusstrasse 1, D-28359 Bremen, Germany[4]

Received 2 December 2009/Accepted 24 November 2010

Four types of titanium (Ti)-based electrodes were tested in the same microbial fuel cell (MFC) anodic compartment. Their electrochemical performances and the dominant microbial communities of the electrode biofilms were compared. The electrodes were identical in shape, macroscopic surface area, and core material but differed in either surface coating (Pt- or Ta-coated metal composites) or surface texture (smooth or rough). The MFC was inoculated with electrochemically active, neutrophilic microorganisms that had been enriched in the anodic compartments of acetate-fed MFCs over a period of 4 years. The original inoculum consisted of bioreactor sludge samples amended with *Geobacter sulfurreducens* strain PCA. Overall, the Pt- and Ta-coated Ti bioanodes (electrode-biofilm association) showed higher current production than the uncoated Ti bioanodes. Analyses of extracted DNA of the anodic liquid and the Pt- and Ta-coated Ti electrode biofilms indicated differences in the dominant bacterial communities. Biofilm formation on the uncoated electrodes was poor and insufficient for further analyses. Bioanode samples from the Pt- and Ta-coated Ti electrodes incubated with Fe(III) and acetate showed several Fe(III)-reducing bacteria, of which selected species were dominant, on the surface of the electrodes. In contrast, nitrate-enriched samples showed less diversity, and the enriched strains were not dominant on the electrode surface. Isolated Fe(III)-reducing strains were phylogenetically related, but not all identical, to *Geobacter sulfurreducens* strain PCA. Other bacterial species were also detected in the system, such as a *Propionicimonas*-related species that was dominant in the anodic liquid and *Pseudomonas*-, *Clostridium*-, *Desulfovibrio*-, *Azospira*-, and *Aeromonas*-related species.

The microbial fuel cell (MFC) (9, 30) is a promising technology for sustainable energy generation, remediation, and sensoring (11, 29, 48, 58). The MFC concept is based on microbial exocellular electron transfer, or the capacity of microbes to transfer electrons produced from the metabolic oxidation of organic substrates to insoluble, extracellular electron-accepting compounds (33, 53). Microbial electron transfer to electrodes can be achieved directly by transferring the electrons produced via bacterial cell membrane cytochromes and protein complexes (37, 44). Alternatively, certain microbes transfer electrons indirectly by the use of environmental or self-produced extracellular electron mediators (3, 18, 27, 34).

Many metal-reducing microorganisms, such as certain Fe(III)-reducing bacteria, have been shown to be electrochemically active in MFC anodic compartments. This is perhaps due to the fact that the solid surface of the electrode resembles the surface of insoluble terminal electron acceptors, such as Fe(III) oxides (2, 7). Fe(III)-reducing bacteria of the *Delta proteobacteria* and specifically members of the *Geobacteraceae* family have been shown to be especially active in MFCs (19, 26), with *Geobacter sulfurreducens* being one of the most extensively studied microorganisms that uses direct electron transfer (2, 45, 52). Other Fe(III)-reducing bacteria have also been detected (19, 32) and isolated (39, 40) from MFCs. However, non-Fe(III)-reducing bacteria can also be active in MFCs (62). Furthermore, bacteria most frequently detected in MFCs are affiliated with *Proteobacteria*, *Firmicutes*, and *Bacteroidetes* (26, 32, 43).

Despite the merits of the MFC as an energy source, MFC technology has not yet been sufficiently optimized for the system to operate as a large-scale application (49, 60). Based on MFC studies so far, some of the most critical factors in optimum MFC operation are the anodic microbial population and its interaction with the electrode surface (33). Materials used as MFC anodic electrodes are characterized by high conductance and chemical stability. Graphite has been used most commonly, in different forms, as anodic electrode core material in MFCs, due to its large current density output (11, 17, 32). Stainless steel (14) and gold (46) were also used as anodic electrodes, but these materials had lower current density outputs than graphite electrodes. Surface-modified electrodes have also been tested in MFCs, in an effort to increase current density output, with positive results. Metal-incorporated and polymer-coated anodic electrodes showed higher activity than their uncoated counterparts (11, 25). In addition, precious-

* Corresponding author. Mailing address: Wetsus, Centre of Excellence for Sustainable Water Technology, Agora 1, P.O. Box 1113, 8900 CC Leeuwarden, Netherlands. Phone: 31 (0) 582 843 180. Fax: 31 (0) 582 843 001. E-mail: urania.michaelidou@wur.nl.

▽ Published ahead of print on 3 December 2010.

metal coating, specifically with platinum (Pt), was shown to increase current density of a graphite electrode almost 20-fold (22).

Despite the good performance of graphite electrodes in MFCs, alternative electrode materials should be explored with the optimization of the MFC process in mind. Titanium (Ti) is preferred in metallurgy for electrode manufacture in dimensionally stable anodes (DSA), mostly because of its chemical stability and hence resistance to deterioration over time (12). This could be a considerable advantage over graphite electrodes for long-term MFC runs. However, Ti is not well studied as anodic electrode core material in MFCs, as it has not been used in MFCs until recently. The current densities of tantalum (Ta)-coated Ti bioanodes were slightly lower than uncoated graphite bioanode current densities (13). In addition, Pt-coated Ti and rough graphite bioanodes exhibited comparable current densities (57), and more recently, Pt-coated Ti electrodes were used in a scaled-up, stacked MFC to produce unprecedented power densities (10). These studies, however, did not address the factor central to MFC energy generation—the bacterial populations attached to the electrode surface(s).

We have studied the relationship between electrode surface properties of different Ti electrodes as bioanodes and performance. The electrochemical performances and major microbial communities of the biofilms of four Ti-based bioanodes were determined. A direct comparison was possible due to the placement of all electrodes tested in the same anodic compartment, where they were exposed to identical growth conditions and microbial populations in the anodic liquid.

MATERIALS AND METHODS

Inoculum source. The anodic liquid (anolyte) was inoculated with electrochemically active organisms from the effluent of a previous MFC run on acetate (55). This mixed culture had been enriched and sequentially transferred from previously run MFC anodes over a period of 4 years (47, 56; R. A. Rozendal, personal communication). The original start-up MFC anode was inoculated with a sludge sample from a full-scale anaerobic paper mill wastewater treatment bioreactor (Eerbeek, Netherlands), anodic effluent from a molasses-fed MFC, and *Geobacter sulfurreducens* strain PCA.

Microbial fuel cell design and setup. The experimental setup consisted of a flat-plate MFC similar to a previously described MFC setup (56). The volumes of the anodic and cathodic compartments were 350 ml each; the total volume of the anolyte, including the recirculation tubing and flow cell, was 650 ml. The anodic and cathodic compartments were separated by a cation-exchange membrane (fumasep FKB; FuMA-tech GmbH, St. Ingbert, Germany). The anodic compartment faced a perspex plate with four vertical channels in which rod-shaped titanium electrodes were placed. The four titanium electrodes (Magneto special anodes B.V., Schiedam, Netherlands) used were identical in shape, macroscopic surface area, and core material; however, they differed in either surface coating or surface texture. These were (i) platinum-iridium composite-coated titanium (Pt-Ti), (ii) tantalum-iridium composite-coated titanium (Ta-Ti), (iii) hydrochloric acid surface-treated titanium (smooth Ti), and (iv) aluminum oxide-blasted titanium (rough Ti). The effective projected macroscopic surface area (height by width) of each electrode was 20 ± 1 cm^2. The four electrodes were connected to the same cathodic electrode. The cathodic electrode was graphite felt (3 mm; FMI Composites Ltd., Galashiels, United Kingdom), with a projected surface area of 290 cm^2. Cathodic and anodic electrodes were connected to the electrical circuit via gold wires.

Microbial fuel cell operation. The MFC was operated at 30°C, and the anodic compartment was continuously fed at a rate of 250 ml/day with a 5 mM potassium acetate-20 mM phosphate buffer solution (pH 7.0), trace minerals, and vitamins as previously described (59). Both the anolyte and the catholyte were recirculated at a flow rate of 10 liters/h. Anolyte pH was controlled at 7.0 with NaOH. Both anodic and cathodic compartments were equipped with Ag/AgCl, 3 M KCl reference electrodes (+205 mV against standard hydrogen electrode). Anodic electrode potentials were collected every 60 s via a Fieldpoint FP-AI-110 module (National Instruments, Woerden, Netherlands). Cell voltages were measured every few days with a multimeter (289true-rms; Fluke Europe B.V., Eindhoven, Netherlands). The MFC was started up with a solution of 20 mM continuously aerated phosphate buffer (pH 7) in the cathode and a resistance (R) of 1,000 Ω for each anodic electrode. After 9 days, the resistance was decreased to 100 Ω. From day 29 to day 33, 50 mM hexacyanoferrate(III) in 20 mM phosphate buffer (pH 7) was used as the catholyte for a fast cathode reaction [reduction of $Fe(III)(CN)_6^{3-}$ to $Fe(II)(CN)_6^{4-}$], and electrochemical tests were performed upon stabilization of the system (see below). On day 33, the catholyte was replaced again with aerated phosphate buffer solution. Operation of the MFC was stopped on day 62.

Electrochemical measurements and data analysis. The anodes were characterized by cyclic and potential-step voltammetry with $Fe(CN)_6^{3-}$ in the cathode (day 29 to day 33 of operation). During cyclic voltammetry, the applied cell voltage, E (V), was cycled from 500 to 700 mV at a rate of 1 mV/s. For potential-step voltammetry, 5 different anode potentials (−450 mV, −425 mV, −400 mV, −375 mV, and −350 mV versus Ag/AgCl) were tested, and the resulting current at the electrode was monitored as a function of time. Each potential was set for 2 min to obtain a stable current; the standard deviation in the current density was always <2% during the last 30 s of the measurements. Current density, J (A/m^2), was calculated based on the projected macroscopic electrode surface area (m^2). Power density, P (W/m^2), was calculated according to $P = E \times J$. All electrochemical tests were performed using a potentiostat (IVIUMstat; IVIUM Technologies, Eindhoven, Netherlands).

Sample collection and enrichments. Biofilm from the electrode surfaces and anolyte samples were collected on day 62. Electrode surface biofilm was aseptically scraped off the entire surface and resuspended in anoxic phosphate buffer (20 mM, pH 7). Subsamples were used to establish enrichment cultures by inoculation into 20-ml serum bottles of anoxic, defined medium as described below, with acetate (10 mM) as the electron donor and nitrate (10 mM) or chelated Fe(III) (10 mM)—in the form of Fe(III) citrate or Fe(III) nitrilotriacetate (NTA)—as the electron acceptor. Enrichments were incubated at 30°C. Growth in enrichments utilizing nitrate as the electron acceptor was monitored visually for turbidity, and enrichments with Fe(III) as the electron acceptor were monitored for Fe(III) reduction, as indicated by color change of the medium from light brown to transparent.

Media for microbial culturing and isolation techniques. Standard aseptic and anaerobic culturing techniques (20, 42) were used throughout. The liquid medium contained the following (g/liter): NH_4Cl (0.25), KCl (0.1), $NaH_2PO_4 \cdot 2H_2O$ (1.56), and $Na_2HPO_4 \cdot 2H_2O$ (1.78). Minerals and vitamins were added (10 ml/liter) from stock solutions as described by Wolin et al. (61), and the pH was adjusted to 7.0 with NaOH. Alternative electron donors and acceptors were added from sterile anoxic stock solutions. Solidified medium for single cell isolation was prepared using the shake agar tube technique (20, 35), with the same medium components amended with 2% (wt/vol) noble agar (Difco). Single colonies were picked from the higher-dilution tubes, and if necessary, isolates were further purified by serial dilutions.

DNA extractions and 16S rRNA gene amplification. Whole-cell DNA was extracted from enrichments and pure cultures using a mini bead beater (Biospec Products Inc., Bartlesville, OK) and a FastDNA Spin kit for soil (MP Biomedicals, Illkirch, France). PCR was performed to selectively amplify the bacterial 16S rRNA gene with primers bact27-f and 1492-r (16) for partial 16S rRNA sequences. The thermocycling parameters were as follows: predenaturation at 94°C for 2 min, followed by 30 cycles of denaturation at 94°C for 30 s, primer annealing at 52°C for 40 s, and elongation at 72°C for 1.5 min. The postelongation step at 72°C was held for 5 min, followed by cooling at 4°C. For denaturing gradient gel electrophoresis (DGGE), bacterial 16S rRNA genes were amplified using primer pair 968-GC-f/1401-r (38). The thermocycling parameters were as follows: predenaturation at 94°C for 5 min, followed by 30 cycles of denaturation at 94°C for 1 min, primer annealing at 56°C for 40 s, and elongation at 72°C for 1 min. The thermocycling postelongation step for DGGE was held at 72°C for 30 min to avoid artifactual double bands (23), followed by cooling at 4°C. Size and yield of the PCR products were estimated by electrophoresis on a 1% (wt/vol) agarose gel. All primers were purchased from MWG-Biotech (Ebersberg, Germany), and PCR buffer, $MgCl_2$ solution, deoxynucleotides, and *Taq* polymerase were purchased from Invitrogen (Breda, Netherlands). The PCR products that were used for sequencing were purified with a NucleoSpin extract II kit (Macherey-Nagel, Düren, Germany).

DGGE and band excision. Amplicons were run on 8% (wt/vol) polyacrylamide gels containing a 30 to 60% denaturant gradient of formamide and urea, as previously described (36). Bands were visualized by silver nitrate staining (51). DGGE bands were excised and incubated in 25 μl of 1× Tris-EDTA buffer (pH 8) at 35°C to extract the DNA. Amplified DNA was run on an agarose gel to

confirm correct amplification and subsequently run on a DGGE gel to confirm purity. Whenever necessary, the band was reexcised and the procedure was repeated until purity was observed. Upon confirmation of a single-band DNA extract, the PCR product was sequenced.

16S rRNA gene sequencing and phylogenetic analysis. 16S rRNA gene amplicons were sequenced using bact27-f and 1492-r (16) and internal primers 519-f and 1100-r (28), whereas amplicons acquired from the single bands extracted from DGGE gels were sequenced with 968-f and 1401-r (28). Sequencing was performed by BaseClear B.V. (Leiden, Netherlands). Sequence fragments were edited and assembled with DNA Baser software and compared against known 16S rRNA gene sequences using the NCBI BLAST tool (http://www.ncbi.nlm.nih.gov/BLAST). Relevant sequences were aligned on the Ribosomal Database Project website (http://rdp.cme.msu.edu/index.jsp) (8). Due to the differences in size of the acquired 16S rRNA gene sequences (bacterial isolates, 850 to 1,383 bp; excised DGGE bands, ~400 bp), the phylogenetic tree was constructed using only the common parts of the aligned sequences (~400 bp). The trimmed sequences were imported into MEGA version 4.0 (54), where the phylogenetic tree was constructed based on the bootstrap consensus tree (15) inferred from 1,000 replicates using the neighbor-joining method (50).

Nucleotide sequence accession numbers. Nucleotide sequences described in this paper were submitted to GenBank under accession numbers GQ463723 to GQ463735.

RESULTS

Start-up of the anodic electrodes. Upon start-up of the MFC, both metal-coated electrodes, Pt-Ti and Ta-Ti, demonstrated similar behaviors: the anode potentials decreased sharply and produced electricity almost immediately. In contrast, the two uncoated Ti electrodes showed a delay of 30 h before producing electricity (i), as shown by the cell voltage (E) in Fig. 1a (where $i = E/R$). The anode potentials versus Ag/AgCl from day 4 to day 8 were -478 ± 2 mV for Ta-Ti, -481 ± 2 mV for Pt-Ti, -424 ± 9 mV for rough Ti, and -404 ± 10 mV for smooth Ti (R = 1,000 Ω). The anode potential values remained at stable levels throughout the experiment whenever the resistance was kept constant or the anodes were not run potentiostatically.

Electrochemical characterization of the bioanodes. During cyclic voltammetry tests, the two metal-coated bioanodes, Pt-Ti and Ta-Ti, showed higher reduction-oxidation activity than the uncoated Ti bioanodes. Power density for all four bioanodes was calculated for corresponding voltages. Performance, expressed as power density at 500-mV cell voltage, decreased in the order Pt-Ti > Ta-Ti > rough Ti > smooth Ti, as shown in Fig. 1b. The Pt-Ti and Ta-Ti bioanodes exhibited high power densities, both approximately 3× and 11× larger than the power densities of the rough Ti and smooth Ti bioanodes, respectively. The power density of the rough Ti bioanode was remarkably higher than that of the smooth Ti bioanode, almost 5-fold. During potential-step voltammetry, the two metal-coated bioanodes produced comparable current densities, up to 5× larger than the uncoated electrode current densities. Again, the bioanode performance decreased in the order Pt-Ti > Ta-Ti > rough Ti > smooth Ti (Fig. 1c).

Major bacterial populations. DNA analyses of the anolyte and the Pt-Ti and Ta-Ti bioanodes indicated several bacterial species present for each sample. Biofilm formation on the uncoated electrodes was poor (as evaluated visually) and insufficient for DNA analyses. Dominant bacterial populations present in the anolyte and on the Ta-Ti and Pt-Ti electrode surface showed comparable patterns between the two electrodes and distinct patterns between the anolyte and the electrodes (Fig. 2a) in each sample. The anolyte contained 14 to 15 dominant species, Ta-Ti showed up to 10 dominant species, and Pt-Ti, which was also the electrochemically best-performing electrode, showed approximately 14 dominant species.

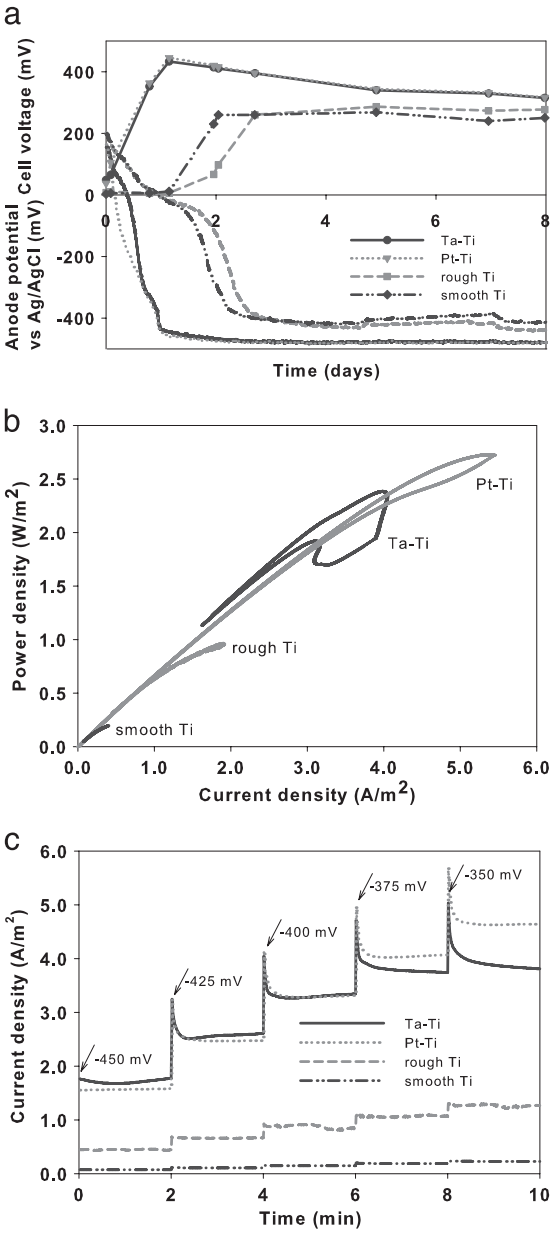

FIG. 1. (a) Cell voltage and anode potential for each electrode (R = 1,000 Ω) during the first 8 days of the microbial fuel cell operation. (b) Power output for each electrode as determined by cyclic voltammetry on an Fe(III)-reducing cathode. (c) Current monitored over time for 25-mV sequential anode potential steps, ranging from −450 mV to −350 mV, for each electrode.

Enrichments and isolates. The enrichments from the two electrochemically best-performing electrodes, Pt-Ti and Ta-Ti, were chosen to be sampled for strain isolation in an effort to acquire dominant and potentially electrochemically active strains from the MFC. Microscopic examination of both the nitrate- and Fe(III)-reducing enrichments (and subsequent transfers) from both electrodes showed the presence of motile, rod-shaped microorganisms. Several acetate-oxidizing, nitrate-

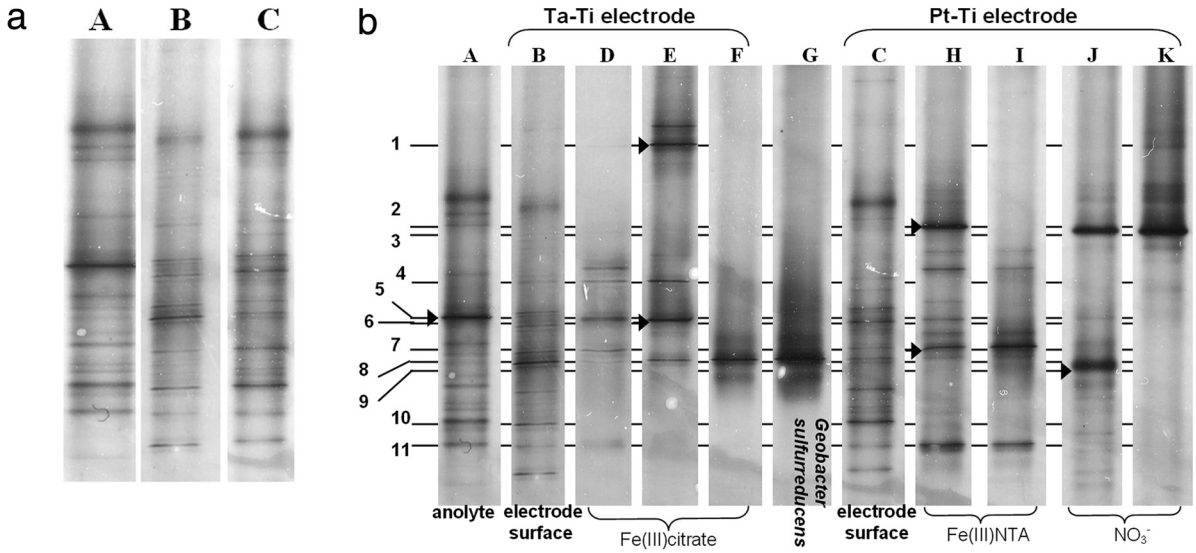

FIG. 2. Dominant bacterial populations present in the MFC analyzed by DGGE, where A indicates the anolyte, B indicates the Ta-Ti electrode surface, and C indicates the Pt-Ti electrode surface. (a) Major acetate-oxidizing populations present in the anolyte and on the surface of each electrode. (b) Comparison of dominant acetate-oxidizing bacterial populations in the anolyte (A), on the surface of the two electrodes (B and C), and in selected Fe(III)-reducing enrichments (D and H), subsequent transfers (E and I), and NO_3^--reducing enrichments (J). The following bacterial isolates are represented: Lac319 (F), T33 (I-7), N968 (K), and reference strain *Geobacter sulfurreducens* PCA (G). Arrowheads at bands A-5, E-1, E-6, H-2, H-7, and J-9 indicate excised bands. Samples were run on a single DGGE gel. The digital image was cropped and minimally edited for brightness and contrast; desired sample lanes were chosen for presentation.

reducing, and Fe(III)-reducing colonies were acquired from the enrichment transfers. Strains N959 and N968 were isolated from nitrate-reducing enrichments of electrode Pt-Ti. Fe(III)-reducing isolates T33 and T32 were isolated from the Fe(III) NTA enrichments of the Pt-Ti electrode. Strains C328, C314, and Lac319 were isolated from the Fe(III) citrate enrichments of electrode Ta-Ti. Strain Lac319 was isolated from a subsequent transfer on lactate of an acetate-oxidizing, Fe(III) citrate-reducing mixed culture.

Dominant Fe(III)- and nitrate-reducing bacteria. Enrichments with complexed Fe(III) compounds as the electron acceptor from biofilm material of the Ta-Ti and Pt-Ti bioanodes indicated several Fe(III)-reducing bacteria present on the surface of both electrodes, as shown by DGGE (Fig. 2b). Ta-Ti biofilm enrichments on Fe(III) citrate indicated up to 8 major Fe(III)-reducing bacterial species (Fig. 2b, lanes D and E). Pt-Ti biofilm enrichments indicated up to 9 major Fe(III)-reducing bacterial species (Fig. 2b, lane H). Some Fe(III)-reducing species were also present as dominant species on the surface of electrode Ta-Ti (Fig. 2b, bands D-7, D-11, and E-8) and electrode Pt-Ti (bands H-6 and H-7). Isolate Lac319 (Fig. 2b, band F-8) and isolates C328 and C314 (not shown) shared the same band position. A band at the same position was also present on the Pt-Ti electrode surface (Fig. 2b, band C-8). Isolates T32 and T33 shared the same band position (Fig. 2b, band I-7) but were not identical to strain Lac319, as indicated by band migration on the DGGE gel. The strains were also present on the surface of both electrodes (Fig. 2b, bands C-7 and B-7). In addition, band positions of Lac319, C328, and C314 suggested that the strains were identical to each other and to reference culture *Geobacter sulfurreducens* (Fig. 2b, band G-8) the organism originally used to enhance start-up of the cell (R. A. Rozendal, personal communication). With the exception of one band (Fig. 2b, band H-2) that was present in Fe(III) NTA enrichments of both the Pt-Ti electrode and the anolyte, other anolyte/bioanode similarities were not detected. Nitrate-reducing communities from the Pt-Ti electrode surface indicated only two dominant species, bands J-3 and J-9 (Fig. 2b, lane J), one of which (band J-3) was similar to isolate N968 (band K-3) (coinciding with the DGGE gel migrating position of isolate N959, not shown on the DGGE gel). These two species at bands J-3 and J-9, however, were not dominant on either one of the electrode surfaces or the anolyte.

16S rRNA gene analysis. Analysis of acquired 16S rRNA gene sequences revealed that the isolates obtained from the enrichments with Fe(III) citrate from electrode Ta-Ti—isolates C328 (1,376 bp), C314 (881 bp), and Lac319 (1,363 bp)—showed, respectively, 99.9%, 100%, and 100% similarity to *Geobacter sulfurreducens* strain PCA. The Fe(III)-reducing bacteria isolated from the Fe(III) NTA enrichments from electrode Pt-Ti—isolates T33 (1,325 bp) and T32 (1,383 bp)—were, respectively, 99.8% and 99.9% similar to an uncultured *Geobacter* species, clone NS1. Similar analysis of the nitrate-reducing strains from the Pt-Ti electrode—isolates N959 (853 bp) and N968 (1,337 bp)—showed, respectively, 100% and 99.2% similarity to *Pseudomonas delhiensis* strain RLD-1. 16S rRNA gene sequence data from DGGE band excision (Fig. 2b) revealed the major bacterial species in the anolyte as a *Propionicimonas paludicola*-related species (99%, band A-5). Other bacterial groups detected by band excision (Fig. 2b) were *Desulfovibrio vulgaris* (98%, band E-6), *Clostridium celerecrescens* (99%, band E-1), *Aeromonas hydrophila* (99%, band H-2) and *Azospira oryzae* (99%, band J-9). Phylogenetic relationships, accession numbers, and known close relatives of isolates and gene sequences identified by excised DGGE bands are shown in Fig. 3.

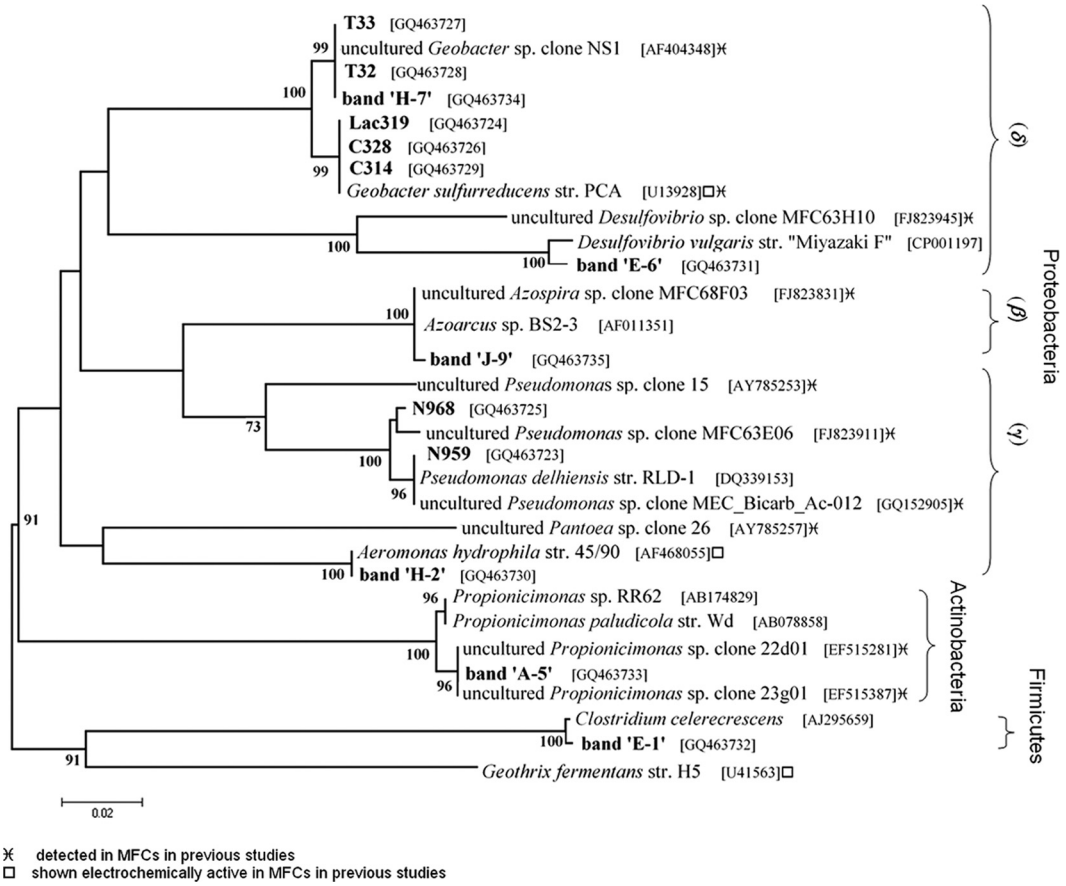

FIG. 3. Phylogenetic relationships, based on 16S rRNA gene sequences of isolates and excised DGGE bands (shown in bold) and close relatives, with bootstrap values of >70% shown. Nitrate reducers N968, N959, and band J-9 and Fe(III) reducers T32, T33, C328, C314, Lac319, and bands E-6, H-7, H-2, and E-1. The cladogram was created using the neighbor-joining method of the MEGA4 application (54). The bootstrap consensus tree inferred from 1,000 replicates was constructed to represent the evolutionary distances of the taxa analyzed.

DISCUSSION

Based on our microbiological studies, the best electrochemically performing bioanodes, Pt-Ti and Ta-Ti, indicated several bacterial species (Fig. 2a) distinct from the anolyte bacterial species. These two bioanodes exhibited some differences in dominant bacterial species, even though both electrodes were exposed to the same microorganisms during operation. This is perhaps an indication of different selection processes of electrochemically active bacteria (EcAB) on the surface of each electrode material. In addition, bacterial species dominant in the anolyte were not present on the surface of the metal-coated electrodes even though planktonic cells in the anolyte might have been in part responsible for some of the electrochemical activity. The uncoated electrode bioanodes, rough Ti and smooth Ti, were the worst electrochemically performing bioanodes and did not produce sufficient biofilm for DNA analysis.

Fe(III)-reducing bacteria, unlike nitrate-reducing bacteria, were abundant on the electrode surfaces analyzed, suggesting the link between the use of Fe(III) and the use of electrodes as extracellular electron-accepting compounds. The Fe(III)-reducing bacteria on the surface of the metal-coated electrodes consisted of *Geobacter* strains, among others. Based on the 16S rRNA gene sequence, isolate Lac319 was phylogenetically identical to *G. sulfurreducens* PCA and was detected on both the Ta-Ti and the Pt-Ti electrode surface. Isolates T33 and T32 were present on the Pt-Ti electrode and were also phylogenetically related to *G. sulfurreducens* (99% similarity in 16S rRNA). They were even more closely related, if not identical, to an uncultured *Geobacter* species, clone NS1, originally detected in quinone-respiring bioreactor enrichments (6). In addition, a clone very closely related (99% similarity in 16S rRNA) to *Geobacter* NS1 was detected in another acetate-fed MFC (26). Detection and isolation of *Geobacter sulfurreducens* strains from the system are not surprising, since the original inoculum was amended with the type strain, a known electrochemically active bacterium. However, it is interesting to see that the strain persisted over the 4-year-long enrichment of EcAB over several MFC transfers.

Bacterial groups other than *Geobacter*, such as *Clostridium*-, *Desulfovibrio*-, *Pseudomonas*-, *Aeromonas*-, *Azospira*-, and *Propionicimonas*-related species, were also detected in this system. Even though these species were not detected as dominant bioanode species in our study, they were also detected in other MFCs of various designs, electrode materials, and growth conditions (Fig. 3). In specific, the species present on the Pt-Ti

electrode (band H-2, Fig. 3) was phylogenetically related to an *Aeromonas hydrophila* strain that was originally isolated from an MFC (40). Moreover, *A. hydrophila* showed high electrochemical activity in MFC inoculum consortia also on Pt-deposited electrodes (22). A *Desulfovibrio* species was previously shown to be active in an MFC using a sulfur electron shuttle (21). Several *Pseudomonas* and *Clostridium* species were also previously detected in MFCs (31, 39, 43), and a variety of *Azospira* clones, related to our detected strain, were also recently acquired from an acetate-fed MFC (4). The dominant species in the anolyte (band A-5, Fig. 3) was very closely related to a group of clones detected in yet another MFC anode (GenBank accession numbers EF515387 and EF515281). These species are related to *Propionicimonas* spp., Gram-positive bacteria in the *Actinobacteria* group (1).

Based on our electrochemical analyses, the four types of titanium (Ti) electrodes exhibited significant differences in performance as bioanodes in the MFC. The Pt-Ti and Ta-Ti bioanodes demonstrated faster and higher cell voltages (and hence higher current production) during start-up (Fig. 1a) than the uncoated Ti (rough and smooth) bioanodes. The differences in cell voltage value between the metal-coated and uncoated Ti bioanodes were most prominent during the first 2 days of start-up; the cell voltages of the two uncoated Ti bioanodes increased perhaps due to the electrochemical activity of planktonic cells and were almost as high as those of the metal-coated bioanodes after day 2. This was most probably due to the slow oxygen reduction rate in the cathode, meaning that the maximum anode potential for each electrode might not have been reached. The differences in current densities of the bioanodes were more clearly seen during voltammetric tests with $Fe(CN)_6^{3-}$ in the cathode for a faster reaction. Cyclic voltammetry scans of bioanodes a month after start-up (power densities shown in Fig. 1b) showed larger current densities of the metal-coated bioanodes than of the uncoated Ti bioanodes. Since the anolyte environment for all four Ti electrodes was the same, the higher current production of the metal-coated electrodes can be explained, at least partly, by the presence of a more substantial biofilm with EcAB formed on the Pt-Ti and Ta-Ti electrodes. Potential-step voltammetry allowed for a more accurate and representative current measurement, and it confirmed best performance of the metal-coated bioanodes, with the Pt-Ti bioanode outperforming the Ta-Ti bioanode (Fig. 1c). The uncoated Ti electrodes produced the worst electrochemically performing bioanodes, due to poor biofilm formation on the Ti surface. Scarce biofilm formation might be explained by the presence of a Ti oxide layer on the surface of the electrode, which has been shown to hinder bacterial attachment (24). In addition, electron transfer to the surface of the electrode might be hindered due to the low conductance of this Ti oxide layer (5). Even so, the rough Ti bioanode produced higher current densities than the smooth Ti bioanode (Fig. 1b and c). This might be explained by a microscopic increase of the electrode surface area after surface blasting and potentially higher numbers of adhered bacterial cells due to lower surface tension and the destruction of the Ti oxide layer.

In conclusion, the higher electrochemical activity of Ti-based bioanodes in MFCs appears to be more related to the precious-metal coating—Pt or Ta—rather than the core material itself. This seems to be due to facilitated bacterial adhesion, since best bioanode performance was linked to biofilm formation. In addition, there might be a bacterial preference for one surface coating over another. This is an important aspect of electrode materials considered for use in large-scale applications, where stable performance is critical. Furthermore, based on the stability of Ti as an electrode, the precious-metal-coated Ti electrodes used in this study are excellent candidates for long-term use and high current production. As demonstrated recently (10), a very high power output, 144 W/m^3, was achieved in a large-scale application using Pt-coated Ti electrodes. It is not yet clear, however, whether the catalytic properties of the metals have an effect on the mode of microbial exocellular electron transfer. Even so, the Fe(III)-reducing bacterial population seems to play a role on the surface of both metal-coated electrodes. It is interesting to compare the physiologies and electrochemical activities of the two different *Geobacte*r strains isolated from the MFC, strains Lac319 and T33, especially since similar species have been detected in other MFCs (26, 32). With the exception of *Aeromonas* and *Clostridium* species, which were previously shown to be electrochemically active in MFC anodes (22, 39), the role of the *Pseudomonas*-, *Azospira*-, and *Propionicimonas*-related organisms in an MFC appears more elusive. These organisms, even though not dominant on the surface of the electrodes in this study, are shown to populate other MFCs, perhaps as auxiliary factors in exocellular electron transfer, such as the production of phenazines or other soluble electron shuttles (41) that can be used by other bacteria. As a result, elucidation of the role of individual microorganisms detected in mixed-culture MFCs is a difficult task. In addition, many of the microorganisms detected in MFCs cannot be tested in MFCs since they exist only as 16S rRNA clone sequence information and were never physically isolated. This fact further highlights the need for MFC *in situ* isolation methods, where EcAB can be isolated and characterized not based on inferred metabolic activities, such as Fe(III) reduction, but based directly on their electrochemical abilities.

ACKNOWLEDGMENTS

We acknowledge financial support by Wetsus and NWO (Chemical Sciences Division of the Netherlands Organization for Scientific Research, grant CW-TOP 700.55.343). Wetsus is funded by the Dutch Ministry of Economic Affairs, the European Union Regional Development Fund, the province of Friesland (Netherlands), the City of Leeuwarden (Netherlands), and the EZ/Kompas program of the "Samenwerkingsverband Noord-Nederland."

We thank Xu Cheng for supplementary data on phylogeny and Astrid Paulitsch, Hauke Smidt, and the participants of the research theme "Energy" for fruitful discussions.

REFERENCES

1. **Akasaka, H., A. Ueki, S. Hanada, Y. Kamagata, and K. Ueki.** 2003. *Propionicimonas paludicola* gen. nov., sp. nov., a novel facultatively anaerobic, Gram-positive, propionate-producing bacterium isolated from plant residue in irrigated rice-field soil. Int. J. Syst. Evol. Microbiol. **53:**1991–1998.
2. **Bond, D. R., and D. R. Lovley.** 2003. Electricity production by *Geobacter sulfurreducens* attached to electrodes. Appl. Environ. Microbiol. **69:**1548–1555.
3. **Bond, D. R., and D. R. Lovley.** 2005. Evidence for involvement of an electron shuttle in electricity generation by *Geothrix fermentans*. Appl. Environ. Microbiol. **71:**2186–2189.
4. **Borole, A. P., et al.** 2009. Integrating engineering design improvements with exoelectrogen enrichment process to increase power output from microbial fuel cells. J. Power Sources **191:**520–527.

5. **Brunette, D. M.** 2001. Titanium in medicine: material science, surface science, engineering, biological responses and medical applications. Springer-Verlag, Berlin, Germany.
6. **Cervantes, F. J., et al.** 2003. Selective enrichment of *Geobacter sulfurreducens* from anaerobic granular sludge with quinones as terminal electron acceptors. Biotechnol. Lett. **25:**39–45.
7. **Chaudhuri, S. K., and D. R. Lovley.** 2003. Electricity generation by direct oxidation of glucose in mediatorless microbial fuel cells. Nat. Biotechnol. **21:**1229–1232.
8. **Cole, J. R., et al.** 2005. The Ribosomal Database Project (RDP-II): sequences and tools for high-throughput rRNA analysis. Nucleic Acids Res. **33:**D294–D296.
9. **Davis, J. B., and H. F. Yarbrough, Jr.** 1962. Preliminary experiments on a microbial fuel cell. Science **137:**615–616.
10. **Dekker, A., A. Ter Heijne, M. Saakes, H. V. M. Hamelers, and C. J. N. Buisman.** 2009. Analysis and improvement of a scaled-up and stacked microbial fuel cell. Environ. Sci. Technol. **43:**9038–9042.
11. **Du, Z., H. Li, and T. Gu.** 2007. A state of the art review on microbial fuel cells: a promising technology for wastewater treatment and bioenergy. Biotechnol. Adv. **25:**464–482.
12. **Duby, P.** 1993. The history of progress in dimensionally stable anodes. J. Miner. Met. Mater. Soc. **45:**41–43.
13. **Dumas, C., R. Basseguy, and A. Bergel.** 2008. DSA to grow electrochemically active biofilms of *Geobacter sulfurreducens*. Electrochim. Acta **53:**3200–3209.
14. **Dumas, C., et al.** 2007. Marine microbial fuel cell: use of stainless steel electrodes as anode and cathode materials. Electrochim. Acta **53:**468–473.
15. **Felsenstein, J.** 1985. Confidence limits on phylogenies: an approach using the bootstrap. Evolution **39:**783–791.
16. **Felske, A., and R. Weller.** 2004. Cloning 16S rRNA genes and utilization to type bacterial communities, p. 523–542. *In* G. A. Kowalchuk, F. J. de Bruijn, I. M. Head, A. D. L. Akkermans, and J. D. van Elsas (ed.), Molecular microbial ecology manual, 2nd ed. Kluwer Academic Publishers, Dordrecht, Netherlands.
17. **Gregory, K. B., D. R. Bond, and D. R. Lovley.** 2004. Graphite electrodes as electron donors for anaerobic respiration. Environ. Microbiol. **6:**596–604.
18. **Holmes, D. E., D. R. Bond, and D. R. Lovley.** 2004. Electron transfer by *Desulfobulbus propionicus* to Fe(III) and graphite electrodes. Appl. Environ. Microbiol. **70:**1234–1237.
19. **Holmes, D. E., et al.** 2004. Microbial communities associated with electrodes harvesting electricity from a variety of aquatic sediments. Microb. Ecol. **48:**178–190.
20. **Hungate, R. E.** 1969. A roll tube method for cultivation of strict anaerobes, p. 117–132. *In* J. R. Norris and D. W. Ribbons (ed.), Methods in microbiology. Academic Press Inc., New York, NY.
21. **Ieropoulos, I. A., J. Greenman, C. Melhuish, and J. Hart.** 2005. Comparative study of three types of microbial fuel cell. Enzyme Microb. Technol. **37:**238–245.
22. **Il Park, H., D. Sanchez, S. K. Cho, and M. Yun.** 2008. Bacterial communities on electron-beam Pt-deposited electrodes in a mediator-less microbial fuel cell. Environ. Sci. Technol. **42:**6243–6249.
23. **Janse, I., J. Bok, and G. Zwart.** 2004. A simple remedy against artifactual double bands in denaturing gradient gel electrophoresis. J. Microbiol. Methods **57:**279–281.
24. **Jeyachandran, Y. L., S. K. Narayandass, D. Mangalaraj, C. Y. Bao, and P. J. Martin.** 2006. The effect of surface composition of titanium films on bacterial adhesion. Biomed. Mater. **1:**L1–L5.
25. **Jiang, D. Q., and B. K. Li.** 2009. Novel electrode materials to enhance the bacterial adhesion and increase the power generation in microbial fuel cells (MFCs). Water Sci. Technol. **59:**557–563.
26. **Jung, S., and J. M. Regan.** 2007. Comparison of anode bacterial communities and performance in microbial fuel cells with different electron donors. Appl. Microbiol. Biotechnol. **77:**393–402.
27. **Kaden, J., A. S. Galushko, and B. Schink.** 2002. Cysteine-mediated electron transfer in syntrophic acetate oxidation by cocultures of *Geobacter sulfurreducens* and *Wolinella succinogenes*. Arch. Microbiol. **178:**53–58.
28. **Lane, D. J.** 1991. 16S/23S rRNA sequencing, p. 115–175. *In* E. Stackebrandt and M. Goodfellow (ed.), Nucleic acid techniques in bacterial systematics. Wiley, Chichester, United Kingdom.
29. **Li, Z., X. Zhang, and L. Lei.** 2008. Electricity production during the treatment of real electroplating wastewater containing Cr6+ using microbial fuel cell. Process Biochem. **43:**1352–1358.
30. **Logan, B. E., et al.** 2006. Microbial fuel cells: methodology and technology. Environ. Sci. Technol. **40:**5181–5192.
31. **Logan, B. E., C. Murano, K. Scott, N. D. Gray, and I. M. Head.** 2005. Electricity generation from cysteine in a microbial fuel cell. Water Res. **39:**942–952.
32. **Logan, B. E., and J. M. Regan.** 2006. Electricity-producing bacterial communities in microbial fuel cells. Trends Microbiol. **14:**512–518.
33. **Lovley, D. R.** 2006. Microbial fuel cells: novel microbial physiologies and engineering approaches. Curr. Opin. Biotechnol. **17:**327–332.
34. **Marsili, E., et al.** 2008. *Shewanella* secretes flavins that mediate extracellular electron transfer. Proc. Natl. Acad. Sci. U. S. A. **105:**3968–3973.
35. **Miller, T. L., and M. J. Wolin.** 1974. A serum bottle modification of the Hungate technique for cultivating obligate anaerobes. Appl. Environ. Microbiol. **27:**985–987.
36. **Muyzer, G., E. C. De Waal, and A. G. Uitterlinden.** 1993. Profiling of complex microbial populations by denaturing gradient gel electrophoresis analysis of polymerase chain reaction-amplified genes coding for 16S rRNA. Appl. Environ. Microbiol. **59:**695–700.
37. **Nevin, K. P., et al.** 2009. Anode biofilm transcriptomics reveals outer surface components essential for high density current production in *Geobacter sulfurreducens* fuel cells. PLoS One **4:**e5628.
38. **Nübel, U., et al.** 1996. Sequence heterogeneities of genes encoding 16S rRNAs in *Paenibacillus polymyxa* detected by temperature gradient gel electrophoresis. J. Bacteriol. **178:**5636–5643.
39. **Park, H. S., et al.** 2001. A novel electrochemically active and Fe(III)-reducing bacterium phylogenetically related to *Clostridium butyricum* isolated from a microbial fuel cell. Anaerobe **7:**297–306.
40. **Pham, C. A., et al.** 2003. A novel electrochemically active and Fe(III)-reducing bacterium phylogenetically related to *Aeromonas hydrophila*, isolated from a microbial fuel cell. FEMS Microbiol. Lett. **223:**129–134.
41. **Pham, T. H., et al.** 2008. Metabolites produced by *Pseudomonas* sp enable a Gram-positive bacterium to achieve extracellular electron transfer. Appl. Microbiol. Biotechnol. **77:**1119–1129.
42. **Plugge, C. M.** 2005. Anoxic media design, preparation, and considerations, p. 3–16. *In* J. R. Leadbetter (ed.), Environmental microbiology, 1st ed. Elsevier Inc., Amsterdam, Netherlands.
43. **Rabaey, K., N. Boon, S. D. Siciliano, M. Verhaege, and W. Verstraete.** 2004. Biofuel cells select for microbial consortia that self-mediate electron transfer. Appl. Environ. Microbiol. **70:**5373–5382.
44. **Reguera, G., et al.** 2005. Extracellular electron transfer via microbial nanowires. Nature **435:**1098–1101.
45. **Reguera, G., et al.** 2006. Biofilm and nanowire production leads to increased current in *Geobacter sulfurreducens* fuel cells. Appl. Environ. Microbiol. **72:**7345–7348.
46. **Richter, H., et al.** 2008. Electricity generation by *Geobacter sulfurreducens* attached to gold electrodes. Langmuir **24:**4376–4379.
47. **Rozendal, R. A.** 2007. Hydrogen production through biocatalyzed electrolysis. Ph.D. dissertation. Wageningen University, Wageningen, Netherlands.
48. **Rozendal, R. A., H. V. M. Hamelers, G. J. W. Euverink, S. J. Metz, and C. J. N. Buisman.** 2006. Principle and perspectives of hydrogen production through biocatalyzed electrolysis. Int. J. Hydrogen Energy **31:**1632–1640.
49. **Rozendal, R. A., H. V. M. Hamelers, K. Rabaey, J. Keller, and C. J. N. Buisman.** 2008. Towards practical implementation of bioelectrochemical wastewater treatment. Trends Biotechnol. **26:**450–459.
50. **Saitou, N., and M. Nei.** 1987. The neighbor-joining method: a new method for reconstructing phylogenetic trees. Mol. Biol. Evol. **4:**406–425.
51. **Sanguinetti, C. J., E. Dias Neto, and A. J. Simpson.** 1994. Rapid silver staining and recovery of PCR products separated on polyacrylamide gels. Biotechniques **17:**914–921.
52. **Srikanth, S., E. Marsili, M. C. Flickinger, and D. R. Bond.** 2008. Electrochemical characterization of *Geobacter sulfurreducens* cells immobilized on graphite paper electrodes. Biotechnol. Bioeng. **99:**1065–1073.
53. **Stams, A. J. M., et al.** 2006. Exocellular electron transfer in anaerobic microbial communities. Environ. Microbiol. **8:**371–382.
54. **Tamura, K., J. Dudley, M. Nei, and S. Kumar.** 2007. MEGA4: Molecular Evolutionary Genetics Analysis (MEGA) software version 4.0. Mol. Biol. Evol. **24:**1596–1599.
55. **Ter Heijne, A., H. V. M. Hamelers, and C. J. N. Buisman.** 2007. Microbial fuel cell operation with continuous biological ferrous iron oxidation of the catholyte. Environ. Sci. Technol. **41:**4130–4134.
56. **Ter Heijne, A., H. V. M. Hamelers, V. Dewilde, R. A. Rozendal, and C. J. N. Buisman.** 2006. A bipolar membrane combined with ferric iron reduction as an efficient cathode system in microbial fuel cells. Environ. Sci. Technol. **40:**5200–5205.
57. **Ter Heijne, A., H. V. M. Hamelers, M. Saakes, and C. J. N. Buisman.** 2008. Performance of non-porous graphite and titanium-based anodes in microbial fuel cells. Electrochim. Acta **53:**5697–5703.
58. **Tront, J. M., J. D. Fortner, M. Plötze, J. B. Hughes, and A. M. Puzrin.** 2008. Microbial fuel cell biosensor for in situ assessment of microbial activity. Biosens. Bioelectron. **24:**586–590.
59. **Van Der Zee, F. P., R. H. M. Bouwman, D. Strik, G. Lettinga, and J. A. Field.** 2001. Application of redox mediators to accelerate the transformation of reactive azo dyes in anaerobic bioreactors. Biotechnol. Bioeng. **75:**691–701.
60. **Watanabe, K.** 2008. Recent developments in microbial fuel cell technologies for sustainable bioenergy. J. Biosci. Bioeng. **106:**528–536.
61. **Wolin, E. A., M. J. Wolin, and R. S. Wolfe.** 1963. Formation of methane by bacterial extracts. J. Biol. Chem. **238:**2882–2886.
62. **Zuo, Y., D. Xing, J. M. Regan, and B. E. Logan.** 2008. Isolation of the exoelectrogenic bacterium *Ochrobactrum anthropi* YZ-1 by using a U-Tube microbial fuel cell. Appl. Environ. Microbiol. **74:**3130–3137.